Interfacing of Ice Load Simulation Tools for Cylindrical and Conical Structure with OneWind simulation tool for offshore wind turbines

Vilho Jussila[1], Wojciech Popko [2] Jaakko Heinonen [1]

[1] VTT Technical Research Centre of Finland, Espoo, Finland

[2] Fraunhofer Institute for Wind Energy and Energy System Technology IWES, Bremerhaven, Germany

ABSTRACT

An offshore wind turbine (OWT) analysis relies on aero-hydro-servo-elastic simulation tools, which take into account an interaction of various environmental conditions and the entire structural assembly of the turbine, including its control system. For the more confident analysis of loads imposed on OWTs located in ice infested regions, an additional interface between sea ice loading and a support structure is necessary.

Two ice load models are interfaced with OneWind, a library for a couple, time domain simulation of OWT developed at Fraunhofer IWES (Strobel 2011). The first model is a procedure for soil-structure-ice-interaction (PSSII) used for vertical structures. The second an ice load model for simulation of the stochastic ice bending failure on a support structure with cone. A simplified OWT with a monopile support structure was considered. The nacelle and rotor assembly was modelled as a point mass at the top. In OneWind an interface for importing ice forces was build. The response of a structure and horizontal ice forces was simulated with PSSII procedure. Then, ice forces are imported with the interface into OneWind, where a structure response is re-simulated. A comparison of the structural response simulated with a standalone PSSII procedure and OneWind produces satisfactory results in terms of displacements. In addition, the difference between the standalone PSSII and OneWind comes from the fact that PSSII is based on modal analysis, whereas OneWind is based on a finite element method. Ice forces on conical support structure are generated by the ice load model and import as well with the interface into OneWind. The structural responses were simulated with Abaqus and OneWind. The comparison of the simulated structural responses shows a good agreement.

Introduction

The popularity of a wind energy production has been expanded to offshore on ice infested regions due to good wind conditions. This process has created a demand to take account ice induced vibration of a structure due to ice action in addition to vibration induced by a wind, wave or combination of both. The focus of this paper is an interface to import ice loads to OWT simulation tool OneWind.

OneWind (Strobel 2011) is a library for a coupled aero-hydro-servo-elastic simulation of OWT in the time domain that is being developed at Fraunhofer IWES. OneWind is based on

Modelica, which is the open-source, object orientated and equation-based language suitable for describing complex systems like OWT. OneWind includes all major components that are necessary for load calculations of current OWT. The library also includes models for environmental conditions, such as wind and waves, and their respective influence on the structures. This research is a step in a sequence started by Heinonen *et al*. (2011) and Hetmanczyk *et al*. (2011) to intergrade additional ice models in OneWind for ice loads simulation on OWT support structures.

The OWT with cylindrical monopile support structure are usually erected for water depths lower than 30 m. The primary failure type of ice field is crushing when the ice field is interacting with cylindrical support structure. Due to the ice-structure interaction the crushing event can be intensive. In such circumstances ice field pushes structure in to the ice drift direction. Suddenly pushing ice field fails releasing energy stored in wind turbine tower and support structure. Consequently structure oscillates respect to the static ice force position. A procedure to investigate ice-structure-interaction is PSSII algorithm developed by Kärnä (1992, 1999). The characterizing feature in PSSII is an ability to simulate ice crushing depending on velocity i.e. intermittent, continuous brittle ice crushing and in addition PSSII is able to simulate lock-in vibration (ISO 19906, 2010).

The ice crushing has been studied widely during preceding decades. One of the earliest is measurements of the continuous brittle ice crushing was carried out on oil drilling platform in Cook Inlet (Blenkarn 1970, Sanderson 1988). Muhonen *et al*. (1992) have carried out ice crushing tests in the ice tank with a freshwater. According to ISO 19906 (2010) classification ice crushing type in the ice tank tests was intermittent. Yue *et al*. (2009) have interpreted results from full scale test on a compliant monopod platform erected in Bohai Bay, China. According the results intermittent, continuous brittle ice crushing and lock-in vibration was observed within the data. One of the earliest concentrated on lock-in vibration phenomenon was Määttänen (1978). Later on, the lock-in vibration was observed by Baker *et al* (2005) in OWT support structure model tests.

OWT with monopile support structures are usually erected for water depths lower than 30 m. Generally monopile wind turbine support structures are considered compliant but the support structure becomes stiffer when it is erected in shallow water. This can be observed from the structural response which decreases conjunctionally with compliances. A compliant structure is prone to severe ice induced vibration.

The support structure can be modified at the water level by installing a cone which reduces ice induced vibration (Baker *et al* 2005). Gravesen *et al*. (2005), Baker *et al* 2005 have studied influences of different cone geometries under ice action extensively. Instead of crushing, the ice field fails by bending. A characterizing feature is a gap formation between ice edge and the structure after the ice failure, Yue *et al*. (2009). In such circumstances the structure vibrates on a vicinity of the low natural frequency respect to neutral position. The purpose of the cone is mitigating ice induced vibrations.

Ralston (1977) has studied static ice forces on sloping structures. Kärnä *et al*. (2004) has modified Ralston (1977) approach by introducing stochastic ice forces and stochastic time depended ice breaking length. Kärnä *et al*. (2004) defined ice breaking length as a function of a first free vibration mode whereas Li *et al*. (2002) has defined ice breaking length from the measurements carried out in Bohai Bay, China.

The objective of this work was creation of an interface for ice models to OneWind library. The interface was utilized to introduce a procedure for soil-structure-ice-interaction tool PSSII used for an OWT cylindrical structure and ice load model for an OWT conical support structure (Kärnä *et al*. 2004, Jussila *et al*. 2012).

Finite element model

In the implementation process the utilized support structure was taken from offshore "NREL 5-MW Offshore Baseline Turbine" (Jonkman *et al*. 2009). The height of the tower is 77.6 m and the submerged part of the monopile was 10 m. Boundary condition at the seabed was assumed fixed. The submerged part of the support structure has a constant radius but tower was tapered from the sea level to the top. In the finite element model tower tapering was modelled with discretized element cross sections. The support structure with cylindrical and conical shape at the mean sea level was constructed with two node linear Bernoulli beams. The contribution of the cone in overall dynamics was taken account with finer mesh at the ice level. The element mass and the moment of inertia were modified to match with physical properties of the cone attached to the support structure. At the top of the support structure a point mass was added, which is equivalent to the mass of the rotor-nacelle assembly of NREL 5-MW turbine (Table 1).

Table 1 Properties of the wind turbine support structure model

	Cylindrical Support Structure model	Conical Support Structure model
Beam Element	2 node, Linear geometrical order with cubic formulation.	2 node, Linear geometrical order with cubic formulation.
Number of Elements	25	24
Radius at ice level [m]	3.00	4.62
Total mass of the model [tonnes]	631	685
Mass of RNA [tonnes]	300	300
Tower [m]	77.6	77.6
Foundation depth [m]	10	10
Foundation boundary condition	Fixed	Fixed
Cone Height [m]	-	5.5
Cone Inclination [deg]	-	60

Dynamics

The approach to solve equation of motion differs depending on the simulation tool. In all simulation tools PSSII, OneWind and Abaqus, the time domain integration was utilized. However, PSSII simulation is based on modal analysis whereas OneWind and Abaqus are based on the finite element method.

The mode superposition method employed with PSSII procedure is based on solution of free vibration mode shapes which is describing linear response of the structure. The wind turbine support structure is a model with a multi-degree-of-freedom (MDOF). The modal superposition has orthogonal property which is used to decomposed coupled equation of motion to series of uncoupled equation of motions Eq. (1) with a single-degree-of-freedom (SDOF) and solved independently. To obtain the solution of equation of motion in the geometrical coordinate system respect to mode shape, the modal displacement response is multiplied by eigenvectors. The final displacement response is obtained with a modal superposition.

$$\ddot{\boldsymbol{U}}_n(t) + \mathbf{C}_n\dot{\boldsymbol{U}}_n(t) + \mathbf{K}_n\boldsymbol{U}_n(t) = \frac{\boldsymbol{R}(t)}{\boldsymbol{M}_n} \quad (1)$$

where $\mathbf{C}_n = 2\boldsymbol{\xi}_n\boldsymbol{\omega}_n$, is a damping as a function of modal damping $\boldsymbol{\xi}_n$ and natural frequency $\boldsymbol{\omega}_n$ [rad/s], $\mathbf{K}_n = \boldsymbol{\omega}_n^2$ is a stiffness, $\boldsymbol{M}_n$ is a generalized mass, $\boldsymbol{R}(t)$ is an ice force [MN], $\ddot{\boldsymbol{U}}_n(t)$, $\dot{\boldsymbol{U}}_n(t)$ and $\boldsymbol{U}_n(t)$ are acceleration [m/s^2], velocity [m/s] and displacement [m] as a function of time [s] in a modal coordinate system.

As shown in Table 1, OWT support structure model with 25 elements including 26 nodes. Due to fixed boundary condition at the seabed 25 nodes with six degree of freedom are participating in the free vibration mode shape solution. Thus, the model has 150 possible free vibration mode shapes. In practice is not convenient include all 150 modes in a simulation with mode superposition. The local mode shapes are becoming more dominant when higher mode shape numbers are considered. A restriction comes from deformation of the structure on each mode. For instance, a linear approximation of one cycle of the sine wave requires 5 nodes, so description of the highest possible mode requires a dense mesh. The localized mode shapes cannot be described correctly with 25 eigenvectors. As shown in Table 2, 40 modes have 94.5 % participation of all mass in a horizontal plane defined by x – and z - axis. On the other hand, if the requirement of adequate number of modes is not fulfilled in the simulation, the missing information of mass and stiffness properties are effecting too much in the solution of the Eq. (1). In a contrast, when considering the solution of equation of motion evaluated with finite element tool, the mass, damping and stiffness matrices in Eq. (2) are defined explicitly.

The sum of modal mass participation gives the total mass involved in the solution of equation of motion in the particular direction (Table 2). In PSSII simulation the equation of motion was solved in a horizontal plane and 40 lowest free vibration mode shapes of 150 were included (Table 2).

Table 2 Mass of model and percentual participation in a horizontal plane in x- and z-directions

	Total Mass	Mass Participation
OneWind model	631 t	100 %
PSSII model - x-axis	596 t	94.5 %
PSSII model - z-axis	596 t	94.5 %

When considering equation of motion utilized by finite element tools OneWind and Abaqus, the response of the structure with MDOF is evaluated with discrete time increments in a geometric displacement coordinates. To obtain the solution the equation of motion is constructed according to Eq. (2).

$$\mathbf{M}\boldsymbol{x}(\ddot{t}) + \mathbf{C}\boldsymbol{x}(\dot{t}) + \mathbf{K}\boldsymbol{x}(t) = \boldsymbol{F}(t) \quad (2)$$

In the Eq. (2) $\mathbf{M}$, $\mathbf{C}$ and $\mathbf{K}$ are mass, damping and stiffness matrices, respectively, $\boldsymbol{F}$ is force vector exciting the motion, $\ddot{\boldsymbol{x}}(t)$, $\dot{\boldsymbol{x}}(t)$ and $\boldsymbol{x}(t)$ are discretize acceleration, velocity and displacement vectors, respectively.
All simulations described here are solving equation of motion as function of time. The difference is the method to obtain acceleration, velocity and displacement at a discrete time step. The time integration in Abaqus and PSSII is based on an extension of the Newmark β method and Newmark method whereas the time integration in the simulations carried with OneWind was based on Euler formulation. The simulation aspects discussed above is collected in the Table 3.

Table 3 Simulation aspects

Structure and tool	Modal coordinate	Geometrical displacement coordinate	Modal Damping	Rayleigh Damping	Time Integration method
cylindrical support structure /PSSII	X		X		Newmark
cylindrical support structure /OneWind		X		X	Euler
conical support structure /Abaqus		X		X	Extension of Newmark β method
conical support structure /OneWind		X		X	Euler

Damping

Rayleigh damping is widely used method in engineering to construct a damping matrix for the equation of the motion solved with finite element tool in the time domain as shown in the Table 3. The simplest method introduces damping in to equation of motion is a proportional damping matrix respect mass or stiffness. However, the common version of the Rayleigh damping is combined damping matrix which is divided in to mass α and stiffness β proportional part (Eq. 4 and 5).

$$\alpha = \frac{2\omega_1\omega_2(\xi_1\omega_2-\xi_2\omega_1)}{\omega_2^2-\omega_1^2} \quad \textbf{(4)}$$

$$\beta = \frac{2(\xi_2\omega_2-\xi_1\omega_1)}{\omega_2^2-\omega_1^2} \quad \textbf{(5)}$$

In the Eq. 4 and 5 control frequencies are ω_1 and ω_2 whereas the corresponding damping factors are ξ_1 and ξ_2. By using Eq. 4 and 5 the combined damping matrix $\mathbf{C}$ in Eq. 2 can be expressed.

$$\mathbf{C} = \alpha\mathbf{M} + \beta\mathbf{K} \quad \textbf{(6)}$$

The mass α and stiffness β proportional Rayleigh damping parameters used in conical support structure simulations are given in the Table 4. The corresponding natural frequencies and damping factors are given as well.

Table 4 Rayleigh damping in cylindrical and conical support structure simulations

Model	α	β	ω_1 [Hz]	ω_2 [Hz]	ξ_1 [%]	ξ_2 [%]
Cylindrical support structure	0.0349	0.0096	0.3618	10.0450	5.0	5.0
Conical support structure	0.0192	0.0009	0.3854	3.5966	0.5	1.0

The simulation in the modal coordinate system with mode superposition provides possibility to define damping for each free vibration mode shape. As stated earlier, PSSII simulation is based on mode superposition, whereas OneWind is traditional finite element tool with a geometric displacement coordinates, hence damping correlation between these coordinate systems were required. One possibility is to simply combine mass α and stiffness β proportional Rayleigh damping equations (Eq. 4 and 5).

$$\xi = \frac{\alpha}{2\omega} + \frac{\beta\omega}{2} \qquad \textbf{(7)}$$

The modal damping in PSSII procedure was approximated in Eq. 1 by using Eq. 7 for each of 40 natural mode shapes. Due to fact that the combined Rayleigh damping is constructed with two control frequencies, the damping ratio as a fraction of critical can be set precisely only for the control frequencies. The cylindrical support structure simulations carried out with PSSII and OneWind, the damping is selected to cover low frequencies as shown in the Figure 1. The selection causes over damping on high frequencies because the stiffness proportional is completely dominating frequencies higher than ω_2 (Eq. 3). The red dots shown in Figure 1 are frequencies used for defining mass α and stiffness β coefficients in the Rayleigh damping. More detailed information is given in Table 4.

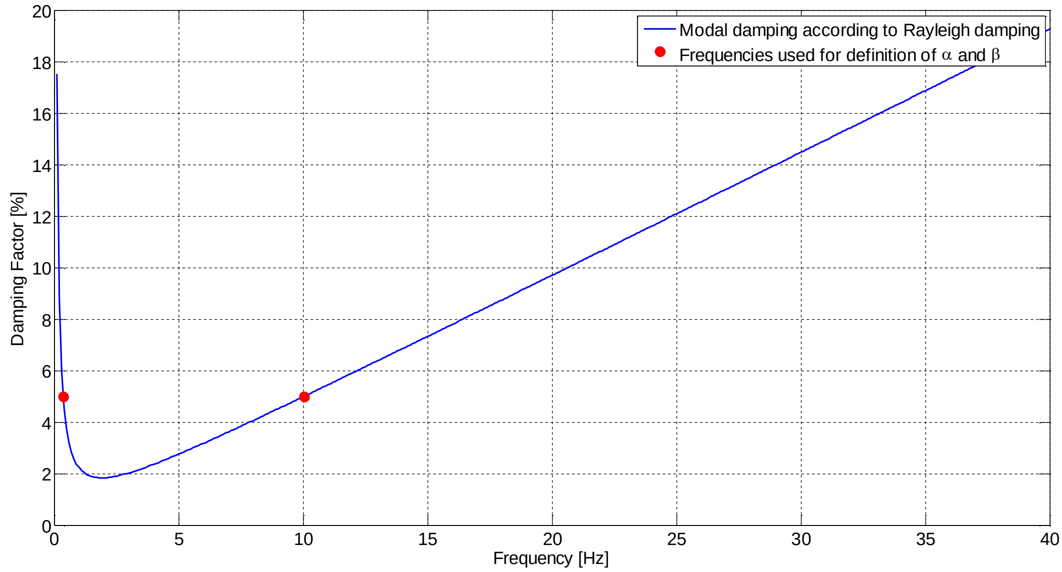

Figure 1 Modal damping used with PSSII

Interface for ice loads

When considering a full implementation procedure of an ice-structure-interaction model such as PSSII, the information of ice loads and structural response on each time step should be interchangeable. This is not the case when the ice load model for conical support structure (Kärnä *et al*. 2004, Jussila *et al*. 2012) is considered. The ice force vector in the ice load model for conical support structure is evaluated without an ice-structure-interaction; hence the response does not effect on ice loads on each simulation time step. Instead of ice-structure-interaction the ice force vector provided by the ice load model for conical support structure is based on normal distribution, ice thickness, velocity and geometry of the structure but not the response of the structure. Hence, the convenient way to implement ice load model for conical support structure is integrate the model as OneWind function which is submitted before solving equation of motion, Eq. 2.

In this case for the sake of simplicity a simple interface was built in OneWind to import ice loads from PSSII or CILM. So, complete simulation loop with PSSII and OneWind has three phases. First, importing solution of free vibration mode shapes to PSSII, second carrying out ice-structure-interaction simulation with PSSII and third importing ice loads to OneWind for further simulations.

Similar approach was used when the simulation loop was carried out with the ice load model for conical support structure and OneWind. However, the simulation loop with the ice load model for conical support structure and OneWind has two phases. First, ice loads are simulated with the ice load model for conical support structure and second the ice loads are imported to OneWind for further simulations.

Structural response comparison

In general, all simulations were carried out with two simulation tools. The cylindrical wind turbine support structure response under ice action was simulated with a standalone PSSII and OneWind. On the other hand the response of the conical wind turbine support structure due to ice induced vibration was simulated with Abaqus and OneWind. Hence, two sets of results were available for comparison.

It is assumed that the cylindrical and conical support structures were erected in 10 [m] deep water and the prevailing ice conditions are as shown in Table 5. As one can recognized, the ice velocity and thickness in the cylindrical support structure simulation with PSSII and OneWind approximates to northern Baltic Sea ice conditions (Tikanmäki *et al* 2012).

In the OneWind simulation carried out with the ice load model for a conical support structure, the ice velocity was chosen according to the breaking length of the ice field. As explained earlier, between adjacent ice loading phases, a gap forms between ice edge and support structure. In the simulation the mean breaking length was 3 m and the standard deviation was 0.4. According to Yue *et al.* (2009), the gap length is 2/3 of the breaking length of the ice field. In these simulations 50 loading phases were generated. The simulation length was set to 100 s. To involve 50 peaks approximately in 100 s, the ice velocity was set to 0.5 m/s.

Table 5 Ice parameters used in the simulations

Model	Ice thickness [m]	Ice velocity [m/s]	Elastic modulus of the intact ice field [MPa]	Bending strength of the ice field [MPa]
Cylindrical support structure	0.5	0.1	3.0	-
Conical support structure	0.6	0.5	-	0.7

Cylindrical support structure simulation results

A displacement response comparison of the cylindrical support structure at the ice level was made between simulations carried out with PSSII and OneWind. According to Figure 2 and simulation results from standalone PSSII procedure and OneWind, a good agreement can be found. A complementary method to study structural response from PSSII and OneWind simulations is the probability density function. This function shows the displacement response from the time history data (Figure 2) on the level axis and number of occurrences on the upright axis. Hence, the probability density function plot shows displacement response distribution (Figure 3). The peak value in the probability density function plot is a mean value of the displacement and represents the deformation under static ice force. In Figure 3 OneWind introduces more occurrences at vicinity of the mean value of displacement and for this reason distribution tails are narrower than the displacement distribution from PSSII simulation. On the other hand, the mean value in the displacement distribution is almost same. As one can observe from Figure 2, displacement response at the ice level in oscillation amplitude is higher respect to the mean value in the results extracted from PSSII simulation than those from the OneWind simulation. This explains differences in the displacement distribution tail width.

The differences in the displacement responses are depending on four sources. First, the solution of Eq. 1 has 5.5 % less mass than the solution of Eq. 2. Second, the damping factor used in the Eq. 1 becomes extremely high when the frequency increases (Figure 1). Third, the stiffness in Eq. 1 is depending on natural frequency which is limited in 40 mode shapes. Fourth, the solver in standalone PSSII and OneWind uses different discrete time integration method. The equation of motion is solved with Newmark direct time integration method in PSSII simulation whereas displacement response was simulated with Euler method in OneWind. Hence, slight differences are coming from modal analysis and finite element approach employed to describe equation of motion.

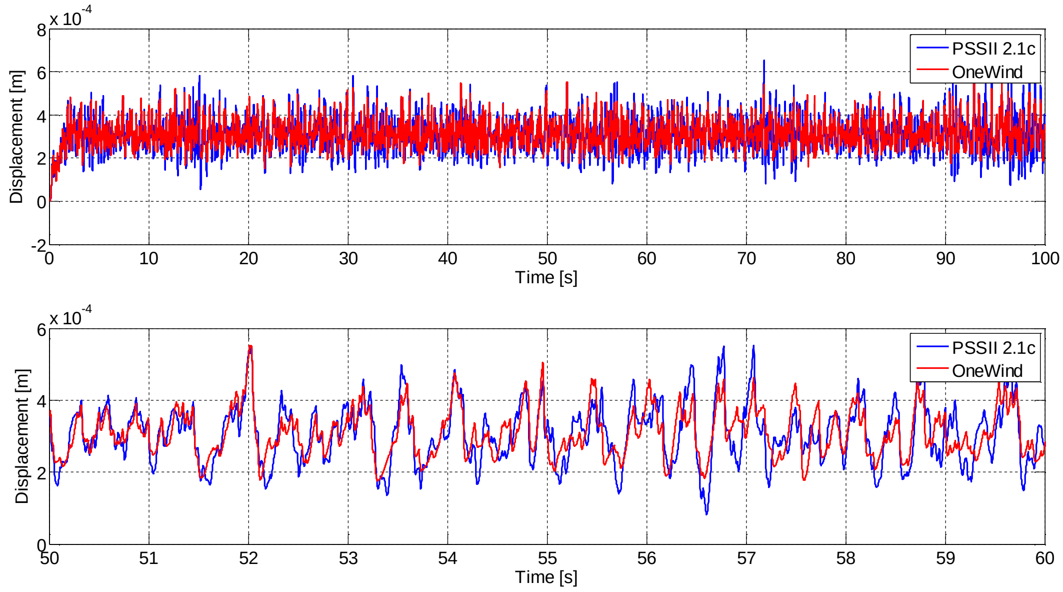

Figure 2 Comparison of cylindrical support structure response at the ice level in time domain

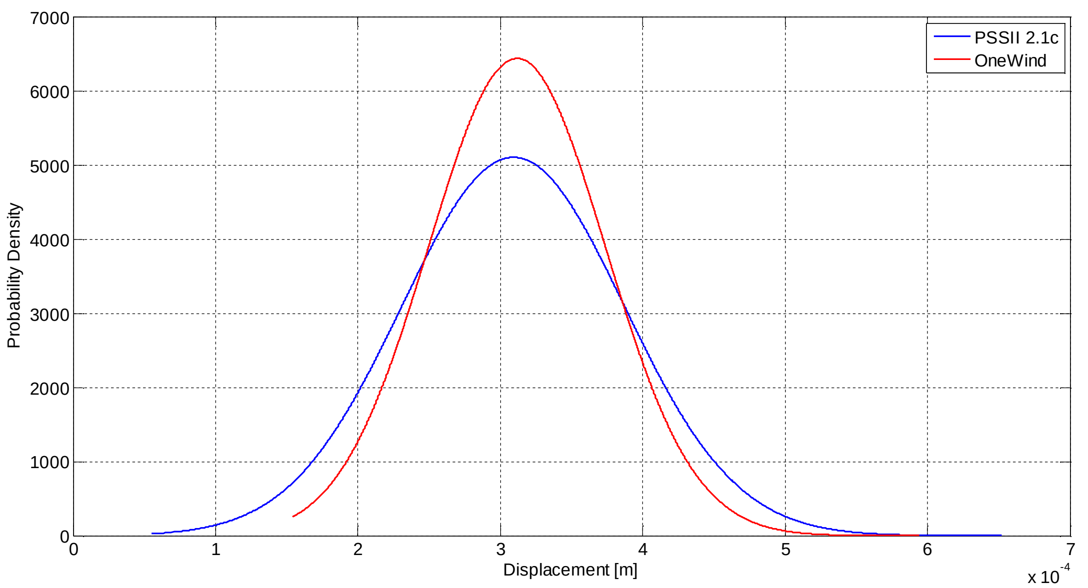

Figure 3 Probability density function plot of structural displacement at the ice level

Conical support structure simulation results

Structural response comparison of the conical support structure under the ice load from CILM was made with OneWind and Abaqus simulations (Figure 4). The displacement response follows with good agreement each other in loading or unloading phase. The loading-unloading phases are the major peak in the time history plot. Between end of unloading and adjacent loading a gap exists between cone and ice edge. This produces a time period of free vibration on lowest natural frequency which can be seen as a low amplitude vibration. The difference between simulation results occurs mainly during the free vibration. This can be observed from Figure 4 as a phase change in vibration. The models in both FEM tools OneWind and Abaqus were identical; hence the slight difference in free vibration is most probably caused by the solver utilized to evaluated solution to equation of motion Eq. 2.

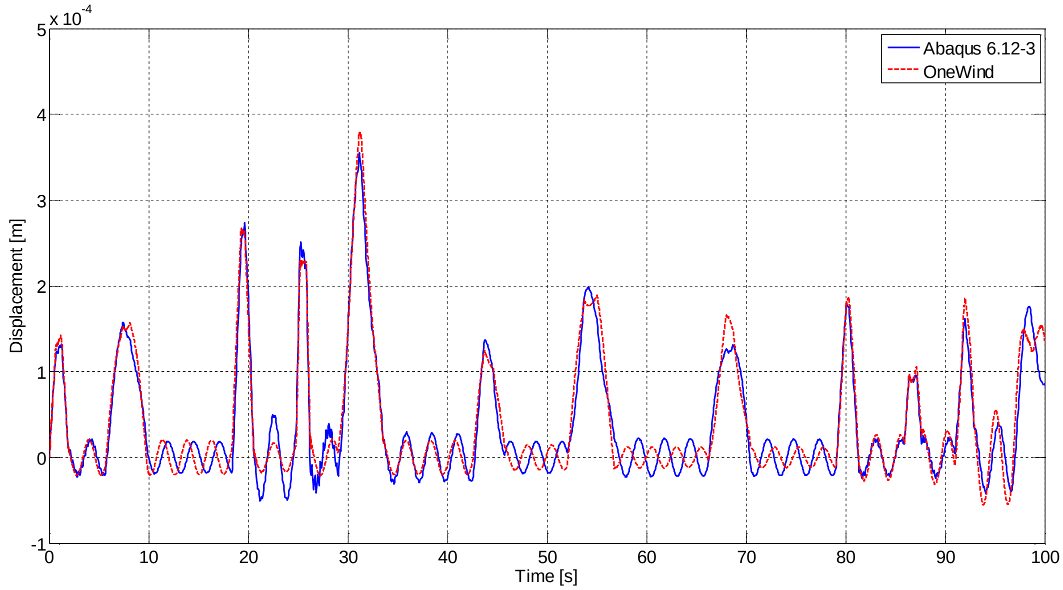

Figure 4 Comparison of structural response from dynamical ice load simulations with Abaqus and OneWind

Conclusion

The objective of this work was creation of the interface for ice models to OneWind library. The interface was utilized to introduce PSSII simulation tool for the cylindrical and ice load model for conical OWT support structures. The interface was tested with a support structure taken from offshore NREL 5 MW baseline wind turbine. In both models cylindrical and conical support structure, the substructure was at the 10 m water depth in the ice infested region.

Conical support structure models were constructed and simulated in Abaqus and OneWind. The ice load used in the simulations was created with the ice load model and imported to Abaqus and OneWind. The result shows good agreement in terms of displacement. However, between adjacent loading phases when a gap between ice edge and the cone is present and the structure is vibrating freely on the lowest natural frequency. It was observed that occasionally the free vibration is out of phase when the simulation results from Abaqus and OneWind was compared (Figure 4). This is caused by different solver algorithms in Abaqus and OneWind.

The simulation of ice-structure-interaction-procedure PSSII with a standalone PSSII and OneWind shows good agreement in terms of structural displacement. According to probability density function plot (Figure 3) the displacement distribution simulated with PSSII is slightly different than the one simulated with OneWind (Figure 3). The differences in the response are due to solution algorithm. The PSSII procedure solves equation of motion on each a time increment with the mode superposition whereas the OneWind is traditional finite element tool in which the equation of motion is solved in time domain with geometric displacement coordinates.

Future Development

The effect of a wind induced vibration on ice forces is should be considered in a model where the solution of equation of motion is based on equilibrium conditions in a time. An ice crushing pressure on each time step in PSSII procedure is depending on relative velocity between ice field and structure. Hence, wind induced vibration effects on the ice crushing pressure but this is considered more in the future development.

References

Barker, A., Timco, G., Gravesen, H., Volund, P., 2005. Ice Loading on Danish Wind Turbines Part 1: Dynamic Model Tests. Cold Region Science and Technology, volume 41, pages 1-23.

Blenkarn, K. A., 1970. Measurements and Analysis of Ice Forces on Cook Inlet Structures. Offshore Technology Conference, Houston, USA, Paper No. 1261, pages 365-378.

Gravesen, H., Sorensen, L., Volund, P., Barker, A., Timco, G., 2005. Ice Loading on Danish Wind Turbines Part 2: Analysis of Dynamic Model Test Results. Cold Region Science and Technology, volume 41, pages 25-47.

Heinonen, J., Hetmanczyk, S., Strobel, M., 2011. Introduction of Ice Loads in Overall Simulation of Offshore Wind Turbines. Proceedings of the 21st POAC International Conference on Port and Ocean Engineering under Arctic Conditions, Montreal Canada.

Hetmanczyk, S., Heinonen, J., 2011. Dynamic Ice Load Model in Overall Simulation of Offshore Wind Turbines. Proceedings of the 21st ISOPE International Offshore and Polar Engineering Conference, Maui, Hawaii, USA.

Jonkman, J., Butterfield, S., Musial, W., 2009. Definition of a 5-MW Reference Wind Turbine for Offshore System Development. Golden, CO: National Renewable Energy Laboratory. NREL Report TP-500-38060.

Jussila. V., Heinonen J. 2012. Comparison of Ice-Induced Vibrations on a Conical and Cylindrical Offshore Wind Turbine Substructure. Proceedings of the 21th IAHR International Symposium on Ice, Dalian China.

Li, F., Yue, Q., 2002. An Analysis of Amplitude and Period of Alternating Ice Loads on Conical Structures. Proceedings of the 16th IAHR International Symposium on Ice, Dunedin, New Zealand, volume 3, pages 87-93.

Kärnä, T. 1992. A Procedure for Dynamic Soil-Strucutre-Ice Interaction. Proceedings of the 2nd ISOPE International Offshore and Polar Engineering Conference, San Francisco, USA, volume 2, pages 764-771.

Kärnä, T. 1993. Rate Effects in Brittle Ice Crushing. Proceedings of the 12th POAC International Conference on Port and Ocean Engineering under Arctic Conditions, Hamburg Germany, volume 1, pages 59-71.

Kärnä, T., Kamesaki, K., Tsukuda, H., 1999. A Numerical Model for Dynamic Ice-Structure Interaction. Computers and Structures 72. pp.645-658.

Kärnä, T., Kolari, K., Heinonen, J., 2004. Mitigation of Dynamic Ice Actions on Offshore Wind Turbines. Proceedings of the Third European Conference on Structural Control, Vienna, Austria.

Li, F., Yue, Q., 2002. An Analysis of Amplitude and Period of Alternating Ice Loads on Conical Structures. Proceedings of the 16th IAHR International Symposium on Ice, Dunedin, New Zealand., volume 3, pages 87-93.

Muhonen, A., Kärnä, T., Eranti, E., Riska, K., Järvinen, E., Lehmus, E., 1992. Laboratory Indentation Tests with Thick Freshwater Ice, volume 1. VTT Research Note 1370, Espoo.

Määttänen, M., 1978. On Conditions for the Rise of Self-Exited Ice-Induced Autonomous Oscillations in Slender Marine Pile Structures. Winter Navigation Research Board, Research Report No 25, Doctoral Thesis.

Ralston, T. D., 1977. Ice Force Design Considerations for Conical Offshore Structures. Proceedings of the POAC International Conference on Port and Ocean Engineering under Arctic Conditions, pp. 741-752.

Sanderson, T. J. O., 1988. Ice Mechanics Risks to Offshore Structures. Graham and Trotman Limited. London, UK. ISBN 0 86010 785 X

Strobel, M., Vorpahl, F., Hillmann, C., Gu, X., Zuga, A., Wihlfahrt, U. 2011. The OnWind Modelica Library for Offshore Wind Turbines – Implementation and First Results Proceedings of the 8th International Modelica Conference, Linköping University Electronic Press.

Tikanmäki, M., Heinonen, J., Makkonen, L. 2012.Estimation of Ice Load Conditions in the Baltic Sea for Offshore Wind Turbine Design. Proceedings of the 21th IAHR International Symposium on Ice, Dalian China.

Yue, Q., Guo, F., Kärnä, T., 2009. Dynamic Ice Forces of Slender Vertical Structures Due to Ice Crushing. Cold Regions Science and Technology, volume 56, pages 77-83.

Yue, Q., Zhang, L., Zhang, W., Kärnä, T., 2009. Mitigating Ice-induced Jacket Platform Vibrations Utilizing a TMD System. Cold Regions Science and Technology, volume 56, pages 84-89.